PHYSICAL REVIEW A **86**, 051602(R) (2012)

Spontaneous symmetry breaking in rotating condensates of ultracold atoms

Armen Sedrakian
Institute for Theoretical Physics, J. W. Goethe University, D-60438 Frankfurt-Main, Germany
(Received 12 May 2012; published 6 November 2012)

We describe an equilibrium state of a rotating trapped atomic condensate, which is characterized by a nonzero internal circulation and spontaneous breaking of the rotational O(2) symmetry with all three major semiaxes of the condensate having different values. The macroscopic rotation of the condensate is supported by a mesh of quantized vortices, whose number density is a function of internal circulation. The oscillation modes of this state are computed and the Goldstone mode associated with the loss of the symmetry is identified. The possible avenues for experimental identification of this state are discussed.

DOI: 10.1103/PhysRevA.86.051602 PACS number(s): 03.75.Kk, 67.85.Hj, 67.85.De

Introduction. Rotating condensates of ultracold Bose or Fermi gases form vortex lattices above a critical rotation frequency. Such states have indeed been observed in a number of experiments on superfluid bosonic [1] and fermionic [2] vapors confined to magnetic and/or optical traps. These systems provide an excellent tool to study various aspects of ultracold rotating atomic gases due to the high level of control over the parameters, such as the number of vortices, strength of interparticle interactions, shape and rotation rate of the trapping potential, multispecies loading of the trap, etc. Various aspects of these rotating condensates have spawned an enormous literature (see, e.g., [3,4]). For our purposes it should be pointed out that theoretical studies of the rotational equilibrium of condensates featuring an array of vortices and their oscillations have confirmed the applicability of "coarse-grained" superfluid hydrodynamics for such systems [5–14]. In particular, an excellent agreement between the theory and experiment is observed for the breathing modes of a uniformly rotating condensate [9]. The applicability of superfluid hydrodynamics needs a sufficiently large and strongly coupled condensate, which can be routinely created in experiments. Under these conditions and in the case of a Bose gas, the quantum pressure term in the Gross-Pitaevskii equations can be ignored compared with the interaction terms, in which case this theory takes the form of superfluid hydrodynamics (see Ref. [5]). Furthermore, the size of the vortex core, which scales with the number of particles as $\xi \sim (8\pi a N)^{-1/2}$, where a is the scattering length, is sufficiently small in this case and need not be resolved.

In this work we explore the rotational state and oscillations of *nonuniformly rotating* condensates. We concentrate on a special class of departures from rigid-body rotation, which feature a constant condensate circulation in the frame rotating with the surface of the condensate. The states that we are seeking are supported by a sufficiently dense mesh of quantum vortices, which guarantee nonzero circulation in the laboratory frame. Bifurcation in condensates at overcritical rotation rates was considered previously with the constraint of irrotationality of the superfluid velocity [15]. Although such states do spontaneously break the rotational symmetry, they are generically unstable and, thus, their time-dependent dynamics is directed towards formation of vortices in the condensate.

We formulate the superfluid hydrodynamics in its virial form, which was proposed and applied previously to uniformly rotating condensates in Refs. [5]. The method has its roots in developments in the context of self-gravitating fluids [16]. There are some parallels (duality), but also differences between gravitationally bound and trapped systems [5]. The states of the condensates discussed below are the duals to the gravitationally bound *Riemann ellipsoids*.

Equilibrium. Consider a rotating cloud of condensed gas confined by a harmonic trapping potential $\phi_{\rm tr}(\boldsymbol{x}) = m\omega_i^2 x_i^2/2$, where m is the atom mass and ω_i are the Cartesian trapping frequency components (hereafter the Latin indices run through 1,2,3–the components of the Cartesian coordinate system–and a summation over the repeated indices from 1 to 3 is assumed). Below we consider the case of axisymmetric trapping with $\omega_1 = \omega_2 \equiv \omega_\perp$. We will assume below that the rotation frequencies are well above the lower critical frequency for nucleation of the vortices, which scales as $\Omega_{c1} \propto (\hbar/mR^2)\ln(R/\xi)$, where R is the size of the condensate transverse to the rotation. Then, the condensate executes rigid-body rotation, where its angular momentum is supported by a vortex lattice. Hydrodynamical treatments of such systems are carried out after averaging (coarse-graining) the dynamical quantities over distances much larger than the intervortex distance. The rotating condensate is then described by the Euler equation, which we write in a frame rotating with some angular velocity $\boldsymbol{\Omega}$,

$$\rho(\partial_t + u_j\nabla_j)u_i = -\nabla_i p - \frac{\rho}{2}\nabla_i\left(\omega_j^2 x_j^2\right) + \frac{\rho}{2}\nabla_i|\boldsymbol{\Omega}\times\boldsymbol{x}|^2 + 2\rho\epsilon_{ilm}u_l\Omega_m, \quad (1)$$

where ρ, p, and u_i are the density, pressure, and velocity of the condensate. We will specify the rotating frame more precisely later on. Equation (1) is valid for Bose or Fermi gases, provided the appropriate equations of state are used. The first moment of Eq. (1), integrated over the condensate volume V, is the second-order tensor virial equation

$$\frac{d}{dt}\int_V d^3x\rho x_j u_i = 2\mathscr{T}_{ij} + \delta_{ij}\Pi + \left(\Omega^2 - \omega_i^2\right)I_{ij} + 2\epsilon_{ilm}\Omega_m\int_V d^3x\rho x_j u_l - \Omega_i\Omega_k I_{kj}, \quad (2)$$

where $I_{ij} \equiv \int_V d^3x\,\rho x_i x_j$ and $\mathscr{T}_{ij} \equiv (1/2)\int_V d^3x\rho u_i u_j$, are the second-rank tensors of the moment of inertia and kinetic energy, and $\Pi = \int_V d^3x p$ is the scalar volume integral of the pressure. A direct integration of the unperturbed hydrodynamic equation for the condensate for the class of

polytropic equations of state shows that the density distribution is of a Thomas-Fermi type, i.e., the density is a quadratic form of the coordinates $\rho = \rho(l^2)$, where $l^2 = x_1^2/a_1^2 + x_2^2/a_2^2 + x_3^2/a_3^2$ [5]. For such a distribution the moment of inertia tensor can be written as $I_{ij} = (4\pi/3)a_i^3 a_k a_l \delta_{ij} \int_0^1 \rho(l^2) l^4 dl$, which will allow us to translate the equations written for moment of inertia tensors to equations written for the semiaxes of the equilibrium condensate.

The equilibrium shape of the condensate in a rotating axisymmetric trapping potential is an ellipsoid of revolution. We fix the origin of the *rotating coordinate system* to coincide with that of the ellipsoid, while the axes of the system coincide with the semiaxes a_1, a_2, and a_3 of the ellipsoid. Thus, the system of coordinates corotates with the axis of the ellipsoid at the frequency $\mathbf{\Omega} = (0,0,\Omega)$ introduced above. We now specialize our discussion to a class of solutions for which $\nabla \times \boldsymbol{u} = \boldsymbol{\zeta}$, i.e., solutions which admit *nonzero vortical motion of the fluid in the rotating frame*. We consider the simplest case of uniform vortical motion along the rotation vector, in which case $u_1 = Q_1 x_2$, $u_2 = Q_2 x_1$, $u_3 = 0$, where Q_1 and Q_2 are constants such that $\zeta_3 = Q_2 - Q_1 \equiv \zeta$. We further assume that the fluid flows associated with internal motions are nonadvective, i.e., satisfy the condition $\boldsymbol{u} \cdot \nabla \rho = 0$, which is manifestly the case for, e.g., incompressible fluids. This implies $u_1 x_1/a_1^2 = -u_2 x_2/a_2^2$ or $Q_1/a_1^2 = -Q_2/a_2^2$, $Q_1 = -a_1^2\zeta/(a_1^2 + a_2^2)$, and $Q_2 = a_2^2\zeta/(a_1^2 + a_2^2)$.

Consider first the stationary solutions of Eq. (2). We write down the diagonal elements of this equation and eliminate Π, to obtain

$$-\omega_3^2 I_{33} = 2\mathscr{T}_{11} + (\Omega^2 - \omega_\perp^2) I_{11} + 2\Omega \int d^3x \rho x_1 u_2$$
$$= 2\mathscr{T}_{22} + (\Omega^2 - \omega_\perp^2) I_{22} - 2\Omega \int d^3x \rho x_2 u_1. \quad (3)$$

Substituting the components of the velocity u_i and after some further manipulations one finds

$$a_1^2 q_\perp^2 = a_2^2 q_\perp^2 = \omega_3^2 a_3^2 + 2\Omega\zeta a_1^2 a_2^2 / (a_1^2 + a_2^2), \quad (4)$$

where $q_\perp^2 \equiv Q_1 Q_2 + \omega_\perp^2 - \Omega^2$, These equalities are satisfied if $\Omega^2 - Q_1 Q_2 = \omega_\perp^2$ and $-2a_1^2 a_2^2 \zeta \Omega/(a_1^2 + a_2^2) = \omega_3^2 a_3^2$. Note that these relations can be equivalently obtained from a variational principle, where the energy of the system is minimized with respect to the parameters a_2 and a_3 at fixed mass, angular momentum, and circulation of the fluid [17]. It is useful to define the ratio $f \equiv \zeta/\Omega$, in terms of which these equilibrium conditions read

$$\bar{\Omega}^2 \left[1 + \frac{\delta_2^2}{(1+\delta_2^2)^2} f^2 \right] = 1, \quad -\frac{2\delta_2^2}{1+\delta_2^2} f \bar{\Omega}^2 = \bar{\omega}^2 \delta_3^2, \quad (5)$$

where the reduced quantities are defined as $\bar{\Omega} = \Omega/\omega_\perp$ and $\bar{\omega} = \omega_3/\omega_\perp$ with $\omega_\perp$ the transverse trapping frequency, $\delta_i = a_i/a_1$, $i = 2,3$, and all the lengths are measured in units of $a_1 = 1$. Equations (5) fully determine the equilibrium structure of the cloud for any pair of values of ζ and Ω. Note that the first equation implies that the rotation frequency must be *below* the transverse trapping frequency, i.e., $\omega_\perp > \Omega$, as is the case also for uniformly rotating condensates. The solutions (5) represent an example of spontaneous symmetry breaking (SSB) in rotating condensed clouds: the initial Lagrangian and the associated hydrodynamical equations have manifest O(2) symmetry, but the ground state does not. Thus, there exists a minimal frequency above which $a_1 \neq a_2 \neq a_3$ as a consequence of $\zeta \neq 0$. Indeed, in the limit $\zeta \to 0$ Eqs. (4) give $(\bar{\Omega}^2 - 1) = \delta_2^2(\bar{\Omega}^2 - 1) = -\bar{\omega}^2\delta_3^2$, which implies that $\delta_2^2 = 1$, $\delta_3^2 = (1 - \bar{\Omega}^2)/\bar{\omega}^2$, i.e., if $\zeta = 0$ the rotational O(2) symmetry is unbroken. The explicit solutions of Eqs. (5) read $\delta_2^2 = (c-1) \pm \sqrt{(c-1)^2 - 1}$, where $c = f^2/2(\bar{\Omega}^{-2} - 1)$ and $\delta_3^2 = -2f\bar{\Omega}^2\delta_2^2/(1+\delta_2^2)\bar{\omega}^2$. Since the radical needs to be positive in order for δ_2^2 to be real, we conclude that there exists a minimum rotation frequency

$$\bar{\Omega} \geqslant \bar{\Omega}_{\min} = (1 + f^2/4)^{-1/2}, \quad (6)$$

above which the SSB sets in.

The energy and angular momentum of the condensate cloud associated with the solutions above are given by

$$E^* = \frac{E}{\omega_\perp^2} = \frac{1}{2}\left[-\left(1+\delta_2^2\right) - \bar{\omega}^2\delta_3^2 \right]$$
$$+ \frac{1}{2}\left(1+\delta_2^2\right)(1+b^2)\bar{\Omega}^2 - 2\delta_2 b \bar{\Omega}^2, \quad (7)$$

$$L^* = \frac{L}{M\omega_\perp} = \frac{1}{5}\left[\left(1+\delta_2^2\right) - 2\delta_2 b\right]\bar{\Omega}, \quad (8)$$

where $b = -f\delta_2/(1+\delta_2^2)$ and M is the mass of the cloud.

Figure 1 shows the values of the (dimensionless) semiaxes of the condensate; for $\Omega < \Omega_{\min}$ only axisymmetric figures exist with $a_1 = a_2 \neq a_3$; for $\Omega \geqslant \Omega_{\min}$ two pairs of nonaxisymmetric solutions exist, which are shown by solid and dashed lines. The figure also shows the energy and angular momentum of these states. It is seen that the solutions with small $(\delta_2, \delta_3 < 1)$ semiaxes have lower energy than the ones with large $(\delta_2, \delta_3 > 1)$ semiaxes in units of a_1. Close to the onset of axial nonsymmetry the energies of both configurations are nearly degenerate, as expected. The velocity fields for

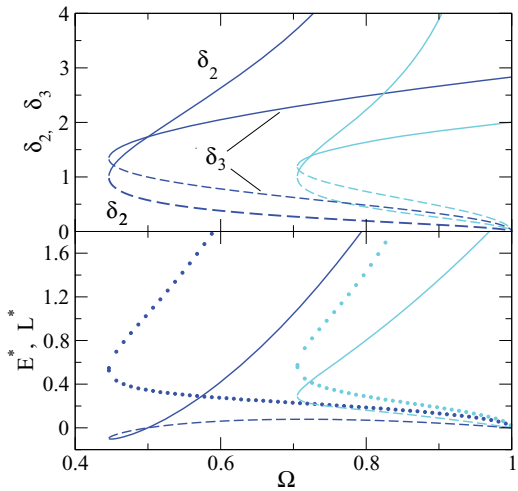

FIG. 1. (Color online) Upper panel: The dimensionless axes δ_2 and δ_3 as functions of the normalized rotation frequency for fixed $f = 4$ (dark, blue online) and $f = 2$ (light, cyan online). The solid and dashed lines distinguish the configurations. Lower panel: The energies of the first (solid lines) and second (dashed lines) configuration for $f = 2$ and $f = 4$. Their angular momenta are shown by dotted lines.

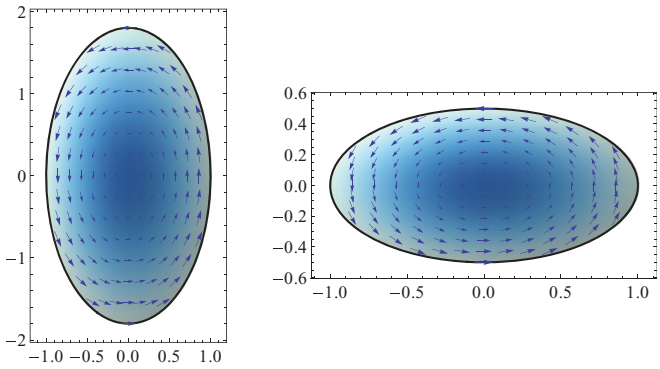

FIG. 2. (Color online) Illustration of the velocity vector field in the x-y plane for two possible solutions with SSB for $\Omega = 0.5$, $f = 4$, and $\delta_2 = 1.8$ (left figure) and $\delta_2 = 0.5$ (right figure). Note that the figures are not to the same scale. The third-axis values are $\delta_3 = 1.5$ and 0.98, respectively. The color coding reflects the Thomas-Fermi density distribution of the cloud.

two possible solutions for fixed values of rotation frequency $\Omega = 0.5$ and circulation $\zeta = 2$ are shown in Fig. 2.

Oscillation modes. Consider small perturbations around the equilibrium with time dependence $\exp(\lambda t)$. The lowest-order nontrivial perturbations are those with $l = 2$ and $|m| \leqslant 2$. The Lagrangian perturbation of Eq. (2) is given by

$$\begin{aligned}&\lambda^2 V_{i:j} - 2\lambda Q_{jl} V_{i;l} - 2\lambda\Omega\epsilon_{il3} V_{l;j} \\ &\quad -2\Omega\epsilon_{il3}(Q_{lk} V_{j;k} - Q_{jk} V_{l;k}) + Q_{jl}^2 V_{i;l} + Q_{il}^2 V_{j;l} \\ &\quad = \Omega^2(V_{ij} - \delta_{i3} V_{3j}) - \omega_i^2 V_{ij} + \delta_{ij}\delta\Pi, \end{aligned} \tag{9}$$

where $V_{i:j} = \int_V d^3x \xi_i x_j$ with ξ_i being the Lagrangian perturbation, and $V_{ij} = V_{i:j} + V_{j:i}$. In the case when the internal circulation $\boldsymbol{\zeta}$ is along the spin vector, the only nonzero elements of the matrices Q and Q^2 are $Q_{12} = Q_1, Q_{21} = Q_2$ and $Q_{11}^2 = Q_1 Q_2, Q_{22}^2 = Q_1 Q_2$. The modes that have even and odd parity with respect to the index 3 decouple. To determine the even modes we need the equation of state of the condensate, which determines the pressure perturbations. For the class of fluids described by a polytropic equation of state $p = \rho^\gamma$ the pressure perturbation is given by $\delta\Pi = (1-\gamma)[(\omega_\perp^2 - \Omega^2)(V_{11} + V_{22}) + \omega_3^2 V_{33}]/2$ [5]. In the case of an incompressible condensate one can proceed in a model- and statistics-independent way, because in that case the perturbations are solenoidal, which translates into $V_{11}a_1^{-2} + V_{22}a_2^{-2} + V_{33}a_3^{-2} = 0$. The characteristic equation for even modes in that case is

$$\mathrm{Det}\begin{pmatrix} \frac{\lambda^2}{2} + p^2 - \Omega Q_2 & -3\Omega Q_1 & -\frac{\lambda^2}{2} - \omega_3^2 \\ +3\Omega Q_2 & \frac{\lambda^2}{2} + p^2 + \Omega Q_1 & -\frac{\lambda^2}{2} - \omega_3^2 \\ a_1^{-2} & a_2^{-2} & a_3^{-2} \end{pmatrix} = 0$$

with the abbreviation $p^2 = \Omega^2 + \omega_\perp^2 - Q_1 Q_2$. In the compressible case the elements in the last row should be replaced: $a_1^{-2} \to (\gamma - 1)(\omega_\perp^2 - \Omega^2)/2$, the same for a_2^{-2}, and finally $a_3^{-2} \to \lambda^2/2 + (1+\gamma)\omega_3^2/2$. Note that the characteristic equation for the modes is invariant under simultaneous interchange $Q_1 \leftrightarrow -Q_2$. Below we assume a Bose gas with $\gamma = 2$. The characteristic equation for even modes is of order 8 in the incompressible case and order 12 in the compressible case. However, the modes come in complex-conjugate pairs and the number of distinct modes is reduced. The odd-parity modes are given by

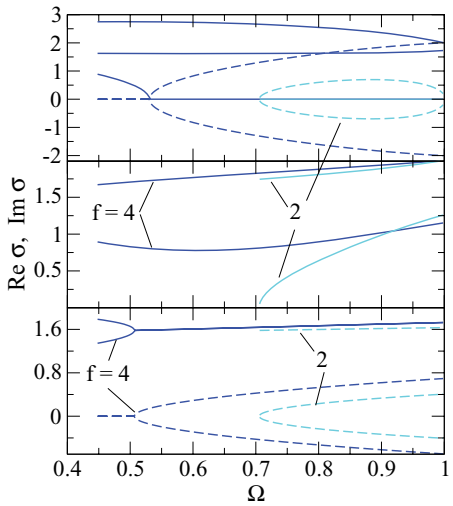

FIG. 3. (Color online) The even-parity compressible (upper panel) and incompressible (middle panel) modes along with the odd-parity (lower panel) modes for $f = 2$ (light, cyan online), and 4 (dark, blue online) as a function of rotation frequency. All quantities are normalized by the transverse trapping frequency $\omega_\perp$. The real parts are shown by the solid lines; the imaginary ones by the dashed lines.

$$\mathrm{Det}\begin{pmatrix} \lambda^2 + \tilde{\omega}_\perp^2 & -2\lambda\Omega & q_\perp^2 - 2\Omega Q_2 & 0 \\ 2\lambda\Omega & \lambda^2 + \tilde{\omega}_\perp^2 & 0 & q_\perp^2 + 2\Omega Q_1 \\ \omega_3^2 & 0 & \lambda^2 + q_3^2 & -2\lambda Q_1 \\ 0 & \omega_3^2 & -2\lambda Q_2 & \lambda^2 + q_3^2 \end{pmatrix} = 0$$

with the abbreviation $q_3^2 = Q_1 Q_2 + \omega_3^2$.

The secular equations for the even and odd modes were solved numerically and their real and imaginary parts are shown in terms of the quantity $\sigma = -i\lambda$ in Fig. 3. The real parts of the σ's are the eigenfrequencies of the modes and their imaginary parts describe their damping. Although for each pair of values of Ω and f there are two equilibrium background solutions which exhibit SSB, there is only one set of oscillation modes associated with both solutions for δ_2 and δ_3. This is consequence of the $Q_1 \leftrightarrow -Q_2$ exchange invariance mentioned above.

There is a trivial undamped odd-parity mode $\sigma_1 = \Omega$, which arises because we are working in the rotating frame. A second undamped mode with eigenfrequency $\sigma_2 = \sqrt{-Q_1 Q_2}$ can be identified with the Goldstone mode, which emerges as a consequence of the SSB; indeed $\sigma_2 \propto \zeta$ and vanishes in the limit where the internal circulation is zero. The remaining odd-parity modes are shown in Fig. 3. There are two physically distinct domains: in the low-rotation-frequency domain there are two real modes without damping; in the high-rotation-frequency domain the real parts are degenerate, whereas the imaginary parts are equal and opposite in sign. The negative imaginary part emerging in this domain indicates *dynamical* (i.e., nondissipative) instability of the system towards

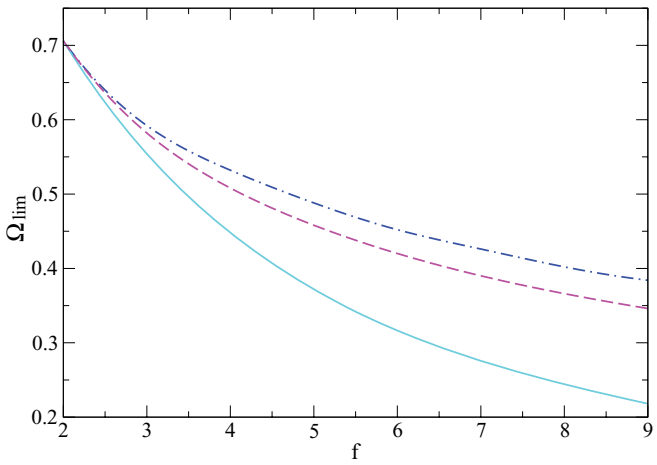

FIG. 4. (Color online) Dependence of the limiting dimensionless rotation rates $\Omega_{\rm lim}$ for onset of SSB, Eq. (6) (above the solid line), for the onset of instability of compressible even modes (above dashed line) and instability of odd modes (above dash-dotted line) on the internal circulation parameter f. The region corresponding to the stable SSB state is enclosed between the solid and the dashed lines.

even-parity oscillations. The two domains are separated by the point of onset of dynamical instability. Furthermore, we see that the stable segment decreases with decreasing f and is absent for $f \leqslant 2$ in our example. There are two real distinct even modes of oscillations in the incompressible case, which are shown in the middle panel of Fig. 3 for $f = 2$, and 4 as functions of rotation frequency. The high-frequency mode weakly depends on the value of f, whereas the low-frequency mode changes its asymptotic behavior in the low-rotation-frequency limit. The incompressible even modes are purely real and correspond to undamped oscillations. The compressible even modes, displayed in the upper panel of Fig. 3, show dynamical instability for high rotation rates, whereby a stable branch of oscillations appears for $f \leqslant 3$ and low rotation rates.

Now we locate the space spanned by the parameters $\bar{\Omega}$ and f, where the SSB state is both energetically favorable and stable against the odd- and even-parity oscillations. In Fig. 4 the region above the solid line, which shows the $\Omega_{\rm lim}(f)$ dependence given by Eq. (6), features the SSB state. This region is bound from above by the minimal frequency at which the even compressible oscillation modes become unstable. Thus, the region between the solid and dashed lines in Fig. 4 corresponds to the parameter space where the SSB state is stable. It is further seen that the minimum frequency at which the odd-parity modes become unstable is larger than that for the even-parity modes for all values of f, i.e., the stability of the SSB state is controlled by the even-parity modes alone.

Experimental verification. The state of rotating condensates with internal circulation can be studied with experimental setups already used for uniformly rotating clouds. First, one needs to establish the SSB by, e.g., measurements of the axis ratio via imaging the condensate. The knowledge of the axis ratios will permit reconstruction of all other parameters of the cloud, including the magnitude of the internal circulation. Second, the number of vortex lines in the cloud can be "counted" again through imaging. Since the equilibrium rotation of the condensate can be independently measured through the excitation of the surface modes, one can detect potential deviations from the Feynman formula $n_v = 2\Omega/\kappa$, where n_v is the number density of vortices and κ is the quantum of circulation. A breakdown of the Feynman formula would be evidence for internal circulations. Indeed, if internal circulations are present then the vorticity in the laboratory frame and the vortex density are given respectively by

$$\zeta_L = (2+f)\Omega, \quad n_v = (2+f)\frac{\Omega}{\kappa}. \tag{10}$$

Thus, a simultaneous and independent measurement of Ω and n_v will give the experimental value of f. Third, the oscillation modes can be measured and tested against theoretical predictions, as has already been done for the $l = 2$ modes of uniformly rotating condensates.

Conclusions. In this work we identified a state of a rotating, harmonically trapped, condensate of an atomic cloud, which in the frame rotating with the cloud's surface has nonzero internal circulation. The resulting equilibrium configurations are nonaxisymmetric, and thus are a manifestation of SSB in superfluid hydrodynamics. We have derived the complete set of $l = 2$ harmonic modes, which are dynamically unstable for high rotation rates and low internal circulation and are stable otherwise. Several experimental tests have been suggested, which can shed light on the structure and small-amplitude oscillations of nonuniformly rotating clouds of Bose and Fermi condensates.

As studies of rotating condensates provide a useful test bed for exploring strongly correlated systems under rotation, due to the great experimental flexibility available in these systems, further insights are expected about systems that are difficult or impossible to manipulate and/or observe. One such example is provided by rotating neutron stars containing strongly interacting condensates of nuclear and quark matter.

Acknowledgments. I am grateful to S. Stringari, H. Warringa, and M. Zwierlein for discussions. I also acknowledge the Aspen Center for Physics, where the major part of this work was done.

[1] M. R. Matthews *et al.*, Phys. Rev. Lett. **83**, 2498 (1999); K. W. Madison, F. Chevy, W. Wohlleben, and J. Dalibard, *ibid.* **84**, 806 (2000); F. Chevy, K. W. Madison, and J. Dalibard, *ibid.* **85**, 2223 (2000); F. Chevy, K. W. Madison, V. Bretin, and J. Dalibard, Phys. Rev. A **64**, 031601 (2001); J. R. Abo-Shaeer, C. Raman, J. M. Vogels, and W. Ketterle, Science **292**, 476 (2001); K. W. Madison, F. Chevy, V. Bretin, and J. Dalibard, Phys. Rev. Lett. **86**, 4443 (2001); E. Hodby, G. Hechenblaikner, S. A. Hopkins, O. M. Marago, and C. J. Foot, *ibid.* **88**, 010405 (2001); P. Engels, I. Coddington, P. C. Haljan, and E. A. Cornell, *ibid.* **89**, 100403 (2002); S. R. Muniz, D. S. Naik, and C. Raman, Phys. Rev. A **73**, 041605 (2006); E. A. L. Henn *et al.*, *ibid.* **79**, 043618 (2009).

[2] M. W. Zwierlein, J. R. Abo-Shaeer, A. Schirotzek, C. H. Schunck, and W. Ketterle, Nature (London) **435**, 1047 (2005); M. W. Zwierlein, A. Schirotzek, C. H. Schunck, and W. Ketterle, Science **311**, 492 (2006); M. W. Zwierlein, C. H. Schunck, A. Schirotzek, and W. Ketterle, Nature (London) **442**, 54 (2006); C. H. Schunck, M. W. Zwierlein, A. Schirotzek, and W. Ketterle, Phys. Rev. Lett. **98**, 050404 (2007).

[3] A. L. Fetter, Rev. Mod. Phys. **81**, 647 (2009).

[4] S. Giorgini, L. P. Pitaevskii, and S. Stringari, Rev. Mod. Phys. **80**, 1215 (2008).

[5] A. Sedrakian and I. Wasserman, Phys. Rev. A **63**, 063605 (2001); **69**, 053602 (2004).

[6] F. Chevy and S. Stringari, Phys. Rev. A **68**, 053601 (2003).

[7] S. Choi, L. O. Baksmaty, S. J. Woo, and N. P. Bigelow, Phys. Rev. A **68**, 031605 (2003).

[8] S. Stock, V. Bretin, F. Chevy, and J. Dalibard, Europhys. Lett. **65**, 594 (2004).

[9] G. Watanabe, Phys. Rev. A **73**, 013616 (2006).

[10] F. Chevy, Phys. Rev. A **73**, 041604 (2006).

[11] G. Watanabe, Phys. Rev. A **76**, 031601 (2007).

[12] M. Antezza, M. Cozzini, and S. Stringari, Phys. Rev. A **75**, 053609 (2007).

[13] E. Lundh and A. Cetoli, Phys. Rev. A **80**, 023610 (2009).

[14] M. Caracanhas, A. L. Fetter, S. R. Muniz *et al.*, J. Low Temp. Phys. **166**, 49 (2012).

[15] A. Recati, F. Zambelli, and S. Stringari, Phys. Rev. Lett. **86**, 377 (2001); S. Sinha and Y. Castin, *ibid.* **87**, 190402 (2001).

[16] S. Chandrasekhar, *Ellipsoidal Figures of Equilibrium* (Yale University Press, New Haven, CT, 1969).

[17] D. Lai, F. A. Rasio, and S. L. Shapiro, Astrophys. J. Suppl. **88**, 205 (1993).